Analog Integr Circ Sig Process
DOI 10.1007/s10470-011-9679-5

Design optimization of an out-of-plane gap-closing electrostatic Vibration Energy Harvester (VEH) with a limitation on the output voltage

R. Guillemet · P. Basset · D. Galayko · T. Bourouina

Received: 25 June 2010 / Revised: 7 December 2010 / Accepted: 21 June 2011

Abstract This paper presents a simple analytical method to optimize the efficiency of an electrostatic out-of-plane gap-closing (OPGC) Vibration Energy Harvesters (VEH). For the first time the electrical and mechanical behaviours of the transducer are addressed simultaneously, while a voltage limitation on the transducer's terminals is set to prevent any damage in the conditioning electronic. The presented work allows to the designer to determine the best strategy depending on whereas the system is passive or able to be self-adapted to the external vibrations parameters. The optimization is performed for a 1 cm^2 device made of bulk silicon to be fabricated using a batch MEMS process. Up to 15 μW can be obtained at 200 Hz if the output voltage is limited to 60 V. The calculations are validated by VHDL-AMS/ELDO simulations.

Keywords Vibration energy harvesting/scavenging · Energy conversion · Electrostatic transduction · Power generation · Microtechnology · MEMS

1 Introduction

The process of electrical power generation from mechanical vibrations involves a mechanical resonator and an electromechanical transducer. It happens in two stages. At first, a proof mass is coupled with the environmental vibrations through an elastic link: the mass and the spring which constitute the resonator are present in almost all mechanical Vibration Energy Harvesters (VEH) (Fig. 1). Thanks to this elastic coupling with the vibrating frame, the mass moves and the resonator accumulates mechanical energy. The second stage consists in the conversion of this mechanical energy into electrical energy. For this purpose, an electro-mechanical transducer has to apply a damping force on the mass, i.e. has to perform a negative work on the mechanical system. A conditioning circuit manages the electrical energy flow so to accumulate the maximum of energy in a reservoir which supplies the load. In addition, the conditioning circuit creates the electrical context necessary for the wanted operation of the electromechanical transducer [1]. This damping force is typically created by magnetic field, straining piezoelectric material or electric field. For a harvester composed of a second order lossless resonator and of an electromechanical transducer of any nature, the absolute upper limit of the power that can be extracted, i.e. converted from the mechanical to electrical domain, is given by [7]:

$$P_{h\ \max} = \frac{1}{2} A_{\text{ext}} \omega m X_{\max} \tag{1}$$

where $X_{\max}$ is the maximal allowed displacement of the resonator mobile mass, m is the resonator lumped mass, ω and A_{ext} are the angular frequency and the acceleration amplitude of the external vibrations respectively. However the transduction mechanism often limits the converted power to a much lower value. For instance, for an electrostatic VEH, the maximal power that can be converted from the mechanical to the electrical domain is given by Meninger et al. [6]:

R. Guillemet (✉) · P. Basset · T. Bourouina
Université Paris-Est, ESYCOM Laboratory, ESIEE Paris, BP 99, 2 bd Blaise Pascal, 93162 Noisy-le-Grand Cedex, France
e-mail: r.guillemet@esiee.fr

D. Galayko
Université Paris-VI, LIP6 Laboratory, BP 167, 4 place Jussieu, 75252 Paris Cedex, France

Published online: 08 July 2011

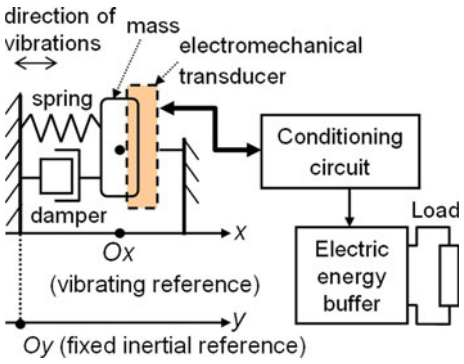

Fig. 1 Diagram of the general architecture of a mechanical energy harvester

$$P'_{h\ \max} = \frac{1}{2} U_0^2 C_{\max} \left(\frac{C_{\max}}{C_{\min}} - 1 \right) f_{\text{elec}} \tag{2}$$

where U_0 is the initial voltage applied on the transducer, $C_{\min}$ and $C_{\max}$ its minimal and maximal capacitance value and f_{elec} the frequency of the transducer capacitance variations. In most existing implementations of electrostatic VEH, the harvested power $P'_{h\ \max}$ is well below the theoretical limit $P_{h\ \max}$. To increase the harvested power $P'_{h\ \max}$, U_0, $C_{\max}/C_{\min}$, and $C_{\max}$ must be maximized. However, several limitations related with the physics and geometry of electrostatic transducer and conditioning electronics impose a restriction on these parameters. The main limitations are the size of the transducer, the electrostatic instability phenomenon and the voltage limitation of the conditioning electronic.

In the present paper we discuss how to optimize the design of the electromechanical resonator of a VEH having an out-of-plane gap-closing (OPGC) architecture [9] and planned to be fabricated using silicon-based microtechnologies. Both mechanical and electrical behaviours of the transducer are taken into account, as well as the specification concerning the maximum voltage allowed by the surrounding electronic. We study the impact of the amplitude's variation of the vibration and we discuss the design strategies depending if the system is passive or includes a dynamic control of the pre-charge. The results are validated with an accurate mixed VHDL-AMS/ELDO model [3] (Fig. 9).

2 Description of the studied device and design issues

2.1 The out-of-plane gap-closing (OPGC) geometry

The structure of an OPGC VEH is represented in Fig. 2. The transducer is composed of two parallel electrodes. One is attached to a rigid frame which is submitted to external vibrations and the other electrode is linked to the frame through a linear spring of stiffness k. When the vibrations

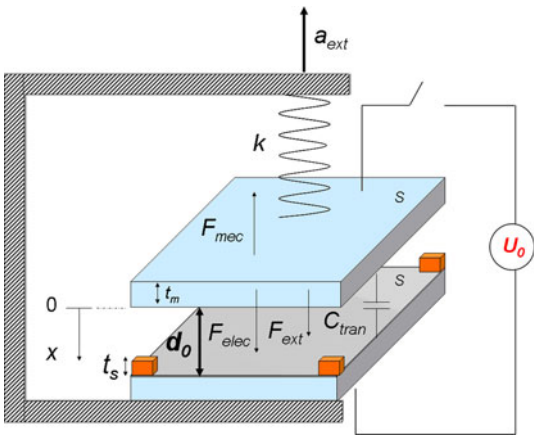

Fig. 2 Representation of an out-of-plane gap-closing VEH

are applied to the frame, the area S of the facing electrodes remains constant: only the gap between them changes due to the external acceleration a_{ext}. Stoppers, made out of an insulating material of thickness t_s, prevent any contact between the two electrodes. The transducer's capacitance C_{tran} is composed of a variable part C_{var} and a constant part C_{par} in parallel to C_{var}. As for any electrostatic VEH, an initial voltage U_0 has to be applied across the transducer's terminals. d_0 is the gap between the electrodes when no voltage or acceleration is applied to the system.

The goal of this study is to identify the fundamental limits of VEH using electrostatic transducer with an OPGC geometry, given reasonable restrictions on the topology for a Si-based MEMS fabrication and on the maximal voltage to be supported by an integrated conditioning circuit. Thus, here we consider a transducer with an area fixed to 1 cm^2; the associated resonator have a mass of 9.3×10^{-5} kg and a stiffness of 147 N/m, which correspond to a natural resonance frequency of 200 Hz. We take C_{par} equal to 10 pF and t_s to 1 µm by default ($= t_{s\ \min}$). The maximal voltage allowed in the system is 60 V. This limit is given by CMOS 0.35 µm technology of Austrian Microsystems, which is a widely used high-voltage CMOS IC technology.

2.2 Dynamic of the VEH mechanical operation

Most of electret-free electrostatic harvesters work at constant charge and their operation is summarized in three steps. Firstly, the electrical (conditioning) circuit put an electrical charge Q_0 on a variable capacitor when its capacitance is at the maximal value $C_{\max}$. Due to the mobile mass motion, the charged capacitor reduces the capacitance to its minimal value $C_{\min}$. Then the capacitor is discharged by the electrical circuit, and in the next semi-period of vibration, the transducer's capacitance increases while being uncharged. According to the formula of electrostatic co-energy stored in the capacitor $W =$

$Q_0^2/(2C_{\text{tran}})$, the discharge energy is higher than the energy spent to charge the capacitor since its capacitance has decreased. The repetition of this ideal cycle generates the average power given by Eq. 2.

To understand the dynamics of the system, one should consider the force $f_t(t)$ generated by the transducer:

$$f_t(t) = \frac{1}{2} U_{C_{\text{tran}}}^2 \frac{\partial C_{\text{tran}}}{\partial x} = \begin{cases} \frac{1}{2}\frac{Q_0}{C_{\text{tran}}}\frac{\partial C_{\text{tran}}}{\partial x}, \frac{\partial C_{\text{tran}}}{\partial t} > 0 \\ 0, \frac{\partial C_{\text{tran}}}{\partial t} < 0 \end{cases}, \quad (3)$$

where $U_{C_{\text{tran}}}$ is the transducer's instantaneous voltage. Given the expression for the transducer capacitance

$$C_{\text{tran}}(x) = \varepsilon_0 \frac{S}{d_0 - x}, \quad (4)$$

the force waveform is a square between 0 and $F_{\max}$:

$$f_t(t) = \begin{cases} F_{\max} = \frac{1}{2}\frac{Q_0^2}{\varepsilon_0 S}, \frac{\partial C_{\text{tran}}}{\partial t} > 0 \\ 0, \frac{\partial C_{\text{tran}}}{\partial t} < 0 \end{cases} \quad (5)$$

Concerning the transducer's design issue, it is more convenient to deal with voltage than with charge. The charge Q_0 is equal to:

$$Q_0 = U_0 C_{\max}, \quad (6)$$

where U_0 is the voltage applied to the transducer when the capacitance is maximal. Since

$$C_{\max} = \varepsilon_0 \frac{S}{d_0 - x_{\max}}, \quad (7)$$

where $x_{\max}$ is the maximum displacement of the mobile electrode. For $F_{\max}$ we have:

$$F_{\max} = \frac{1}{2} U_0^2 \frac{\varepsilon_0 S}{(d_0 - x_{\max})^2}. \quad (8)$$

Hence, the transducer's force waveform is only determined by the transducer's geometry, the initial precharge voltage and the maximal displacement of the mobile electrode. This will allows to consider $x_{\max}$ as a "free parameter" in further analysis, and to express other dynamic parameters through it.

The analysis presented in this paper is based on the assumption that in the steady state operation, the motion of the resonator is sinusoidal, even if the forces applied on the mass are not. This assumption is justified by the passband characteristics of the resonator, which selects the first (fundamental) harmonic of the force, filtering the higher harmonics. In this analysis, two components of the mobile mass position (x) are considered: the zero frequency harmonic (the average position) and the fundamental harmonic.

First, we find the average position of the resonator: for this, the average force applied by the transducer must be determined. Since the transducer has a monotonous $C_{\text{tran}}(x)$ characteristic, the time derivative is negative exactly a half of each periodic cycle, hence, the average force is $F_{\max}/2$. Since this average force is applied to a spring, the average position is

$$x_{\text{med}} = \frac{F_{\text{elec\_max}}}{2k} = \frac{1}{4} U_0^2 \frac{\varepsilon S}{(d_0 - x_{\max})^2}. \quad (9)$$

The sinusoidal component of the motion depends as well on $F_{\max}$, on the external vibrations and on the resonator's mechanical impedance [4, 5]. In this paper we are not interested in calculation of the exact amplitude of the resonator motion given all these parameters, but rather in identification of fundamental limitations imposed by the various constraints mentioned previously.

2.2.1 *Relation between the displacement's amplitude and the maximal converted power*

The maximal convertible power $P'_{h\ \max}$ is determined by the maximal and minimal transducer capacitances: C_{tran} takes extreme values when the mobile electrode is at extreme positions $x_{\max}$ and $x_{\min}$. Since the motion is assumed sinusoidal, $x_{\min}$ is situated symmetrically with $x_{\max}$ with regard to x_{med} and is equal to:

$$x_{\min} = 2x_{\text{med}} - x_{\max} \quad (10)$$

From $x_{\min}$, $C_{\min}$ can be calculated similarly with (Eq. 7), and the power $P'_{h\ \max}$ can be expressed through $x_{\max}$, U_0 and the resonator's geometric parameters.

2.2.2 *Limitations related with instability issues*

In the constant-charge harvesting scheme, the instability phenomenon can be explained as following. During the motion, once the variable capacitance reaches the maximal value, a voltage U_0 is applied on it. The maximal capacitance corresponds to the maximal displacement $x_{\max}$ of the mobile mass: at this position, the mobile mass velocity is zero, and the only force opposing to the electrostatic force is the spring's force $kx_{\max}$.[1] If this force is less than the force $F_{\max}$, then the mobile mass will be attracted to the fixed transducer's electrode and a dynamic pull-in will take place. Hence, $x_{\max}$ is limited not only by the stopper position, but also by the pull-in phenomenon. In the next paragraph we analyze this issue and deduce a first limitation on $x_{\max}$.

[1] In reality, there is a third force: the "external acceleration" equivalent force ma_{ext}, which can be oriented so to push the resonator to its equilibrium position. However, depending on the relation between the resonance frequency of the system and the external vibration frequency, the phase shift can be such that this force is zero when $C_{\text{tran}} = C_{\max}$ (e.g., at the resonance frequency). We suppose this "worst case" in this analysis.

It is known that for our device biased by a fixed voltage U_0, the limit of static stability is given by the couple $\{U_{pi}, x_{pi}\}$ which is equal to $\left\{\sqrt{\frac{8kd_0^3}{27\varepsilon S}}\frac{d_0}{3}\right\}$. Here U_{pi}, called "pull-in voltage", is a minimal voltage at which no equilibrium point exists for the resonator, [i.e., for $U_0 > U_{pi}$, the electrostatic force f_t is superior to kx for all x in $(0, d_0)$], and $d_0/3$ is the maximal (limit) value of the equilibrium position corresponding to U_{pi} [8]. However, if U_0 is lower than U_{pi} the system has two equilibrium points: one stable and one unstable, situated at $x_{\text{eq stable}}$ and $x_{\text{eq unstable}}$ so that $d_0 > x_{\text{eq unstable}} > d_0/3 > x_{\text{eq stable}} > 0$ (Fig. 3). For a given pre-charge $U_0 < U_{pi}$, any position of the mobile electrode lower than $x_{\text{eq unstable}}$ backs off to the stable position and any position higher than $x_{\text{eq unstable}}$ collapses to $x = d_0$ or, if stoppers are present, to $d_0 - t_s$. Hence, the resonator's mobile mass position should never exceed $x_{\text{eq unstable}}$: this imposes a natural limitation on $x_{\max}$. Note that $x_{\text{eq stable}}$ is not the same as x_{med}: the former is the equilibrium position in the static mode, the latter is determined for the dynamic mode, and they are not equal since the system is nonlinear.

The value of $x_{\text{eq unstable}}$ can not be found analytically, since it is a root of the following third order polynomial equation:

$$kx_{\text{eq\_unstable}} = \frac{1}{2}U_0^2\frac{\varepsilon_0 S}{\left(d_0 - x_{\text{eq\_unstable}}\right)^2} \tag{11}$$

$x_{\text{eq unstable}}$ reduces when the voltage U_0 increases. $x_{\text{eq unstable}}$ defines the maximal value of $x_{\max}$ and $x_{\min}$, hence, the value of $C_{\max}$ and $C_{\min}$ and hence, the value of the harvested power $P'_{h\ \max}$.

According to (Eq. 2) there are two ways of maximizing $P'_{h\ \max}$:

1. to work with a large value of U_0. However in this case, the average and unstable equilibrium positions are close, which limits the excursion of the mobile plate and leads to a smaller $C_{\max}$ and $C_{\max}/C_{\min}$ ratio, and $P'_{h\ \max}$ actually decreases.
2. to pre-charge the system with a low U_0: the unstable equilibrium is close to the fixed electrode and a large mobile electrode displacement is possible which allows to maximize $C_{\max}$ and $C_{\max}/C_{\min}$ ratio. But the conditioning circuit designer may have to deal with high voltages when collecting the high-energy charges at the $C_{\min}$ position (cf. Eq. 12).

As we will show in the next section, the choice of U_0 has to be carefully chosen for a given d_0, and if a limit is set on the transducer's output voltage, there is always an optimum couple $\{U_0, d_0\}$.

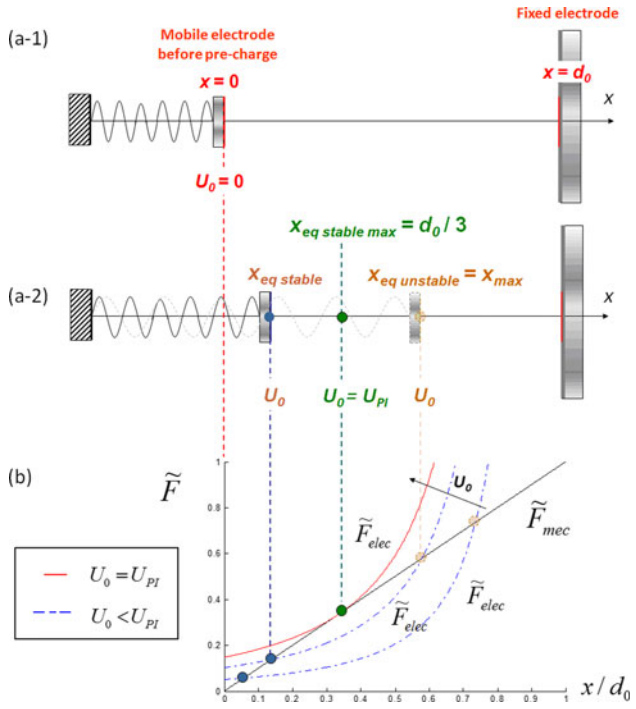

Fig. 3 Position of the mobile electrode without any applied voltage $(a - 1)$ and equilibrium positions for $U_0 \neq 0$ $(a - 2)$. Representation of electrostatic and mechanical forces as a function of the displacement of the mobile plate and U_0 (b)

3 Design optimization with a limitation on the output voltage

Figure 4 shows the evolution of the maximal harvested power $P'_{h\ \max}$ calculated from (Eq. 2) versus U_0 and for designs varying the initial gap d_0 between the transducer's electrodes. For a given $\{U_0, d_0\}$, $C_{\max}$ and $C_{\min}$ are calculated respectively as the transducer's capacitances C_{tran} at the $x_{\max} = \max(x_{\text{eq unstable}}, d_0 - t_s)$ and $x_{\min}$ positions. It is supposed that the external vibrations amplitude and the resonator's mechanical impedance value allow exactly this maximal displacement. As the voltage U_0 decreases, $x_{\text{eq unstable}}$ goes closer to the fixed electrodes, and from a certain value of U_0, becomes beyond the stoppers. For each curve, the maximum of $P'_{h\ \max}$ corresponds to the highest value allowed for the $C_{\max}/C_{\min}$ ratio, i.e. when the mobile plate reaches the stoppers at $x_{\max} = d_0 - t_s$. From these curves, it appears that to get a maximum of converted power, it is better to work with a design allowing a large displacement of the mobile mass than a large pre-charge voltage. However, another major limitation comes from the voltage allowed across the transducer's terminals that should not be destructive for the surrounding electronic.

The problem of the high voltage on the transducer can be explained as follows. As the transducer is charged with a

charge Q_0 when its capacitance is maximal, the voltage across its two electrodes $U_{C_{\text{tran}}}$ is defined by:

$$U_{C_{\text{tran}}} = \frac{Q_0}{C_{\text{tran}}} = U_0 \frac{C_{\max}}{C_{\text{tran}}} \tag{12}$$

Its maximal value $U_{C_{\text{tran max}}}$, which appears at $C_{\text{tran}} = C_{\min}$, is represented in Fig. 5 versus the pre-charge voltage U_0 and for various values of d_0. As in Fig. 4, for each point of these curves, the mobile mass is supposed to travel between $\min(x_{\text{eq unstable}}, d_0 - t_s)$ and the corresponding $x_{\min}$. Except for high values of d_0, the $C_{\max}/C_{\min}$ ratio decreases faster than U_0 increases, consequently $U_{C_{\text{tran max}}}$ decreases similarly at constant d_0.

High-voltage IC technologies don't allow voltages above 100 V and typical maximum voltage is around 50 V. Since we target to implement our smart conditioning circuit in the high voltage CMOS 035 µm technology from Austrian Microsystems, we fixed $U_{C_{\text{tran max}}}$ at 60 V. Then, the allowed range of couples (U_0, d_0) is given in the zoomed area in Fig. 5. From this plot and from Fig. 4, it is possible to find an optimal couple (U_0, d_0) maximizing the harvested power. Using *Optimtool* of *Matlab*, we obtained the parametric plot in Fig. 6 representing the highest harvestable power versus $U_{C_{\text{tran max}}}$, both calculated in function of U_0 and d_0. As in previous plots, each $U_{C_{\text{tran max}}}$ corresponds to the voltage generated on C_{tran} when the displacement corresponds to $x_{\max} = \min(x_{\text{eq unstable}}, d_0 - t_s)$.

The dotted part of each curve is associated to low values of U_0 and corresponds to $x_{\text{eq unstable}}$ being beyond the stoppers: $x_{\max}$ is then located at the stopper position $d_0 - t_s$. Hence, the allowable traveling of the mass is constant for all U_0 in this range, and $C_{\max}$ and $C_{\max}/C_{\min}$ remains constant at its maximum value corresponding to $x_{\max} = d_0 - t_s$. Under these conditions, $P'_{h\ \max}$ increases

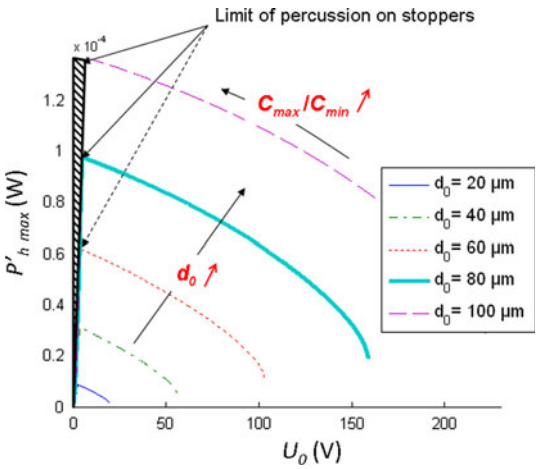

Fig. 4 Variation of $P'_{h\ \max}$ as a function of U_0 for various values of d_0

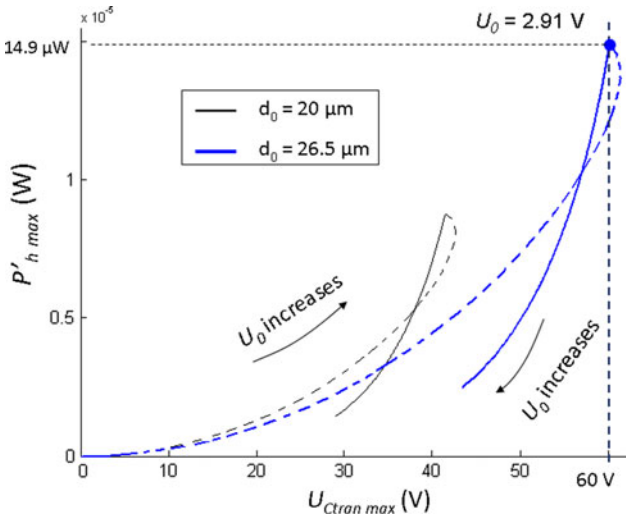

Fig. 6 Evolution of $P'_{h\ \max}$ as a function of $U_{C_{\text{tran max}}}$ for various values of d_0

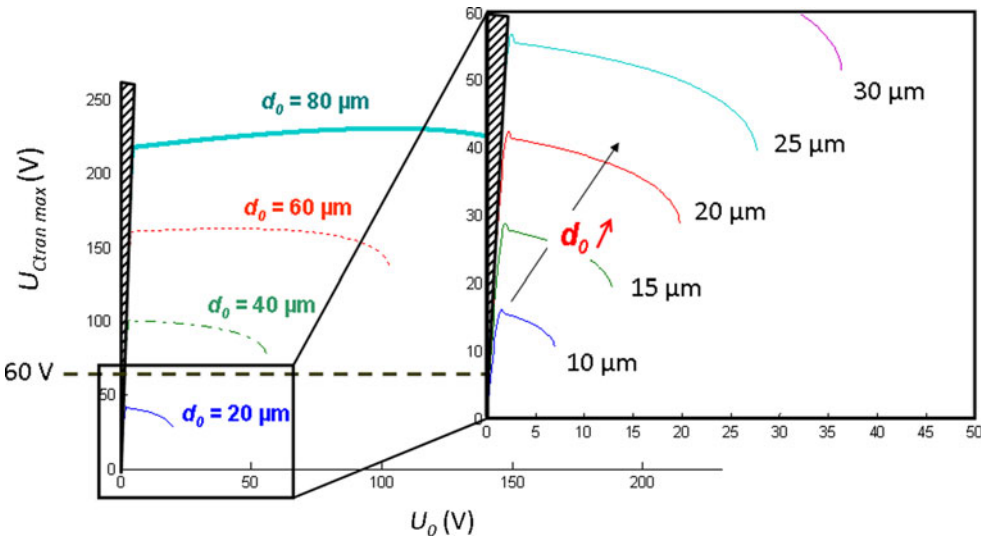

Fig. 5 Representation of the maximal voltage across the capacitance $U_{C_{\text{tran max}}}$ as a function of U_0 for various values of d_0

proportionally to U_0^2. The top of curves corresponds to the optimum pre-charge when $d_0 - t_s = x_{\text{eq unstable}}$. From this point, any increase of U_0 decreases $P'_{h\ \max}$ since $x_{\text{eq unstable}}$ and then $C_{\max}/C_{\min}$ decrease. If a voltage limitation is set, this extremum has to fit with it in order to maximize the harvested power. For instance, for our example, the best design is with a gap $d_0 = 26.5$ µm and a pre-charge of 2.91 V, leading to a maximal harvested power of 14.9 µW. In these conditions, the $C_{\max}/C_{\min}$ ratio is 895/43 pF $\sim$ 20.

3.1 Consequences of a variation of the vibration's amplitude

In this paragraph we study the impact of a 10% reduction of the mobile electrode displacement due to a decrease in the external acceleration for a given design. In the case when the optimal $x_{\max}$ is very close to d_0, an amplitude decrease (i.e., $x_{\max}$ decrease) implies a dramatic decrease of $C_{\max}/C_{\min}$, considering (Eq. 4):

$$\frac{C_{\max}}{C_{\min}} = \frac{d_0 - x_{\min}}{d_0 - x_{\max}} \tag{13}$$

This leads to a smaller $C_{\max}/C_{\min}$ ratio for which the device's design is no more optimal. From the harvested power optimization point of view, it is equivalent to say that the stopper's thickness t_s is now 3.5 µm instead of 1 µm. Compared to figures obtained in the preceding section, the highest $C_{\max}/C_{\min}$ ratio becomes 259/29 pF $\sim$ 9. The impact of such a vibration change is illustrated in Fig. 7 with the dotted curve. The second half of the curve fits with the previous case since d_0 is the same and the mobile electrode doesn't reach the stopper's position. If U_0 is maintained at the same level, the new maximal harvested power dramatically decreased to $P'_{h\ \max} = 1.77$ µW, namely a decrease of almost 90%, which is disastrous for the energy harvesting process. However if after this amplitude change the pre-charge can be adjusted to its new optimal value of 10 V, the $C_{\max}/C_{\min}$ ratio becomes 6, and the harvested 12.3 µW for a maximum output voltage of 58.5 V.

Consequently there are two approaches to limit the impact of the vibration's amplitude variations:

1. to have a smart system where the pre-charge can be adjusted to the fluctuation of the external acceleration during the conversion process. Such architecture has been proposed by Dudka et al. [2].
2. to limit the transducer's sensitivity. This can be obtained with thicker stoppers, leading to a smaller value of $C_{\max}$, and then to a smaller $C_{\max}/C_{\min}$ ratio.

For instance we can choose to design a transducer with $C_{\max}/C_{\min} = 4$. The design optimisation gives the following parameters: $d_0 = 27.4$ µm and $U_0 = 15$ V and the stoppers thickness is $t_s = 5.6$ µm. The maximal harvested power $P'_{h\ \max}$ is almost 11.4 µW for $U_{C_{\text{tran max}}} = 60$ V. If the mobile electrode displacement is reduced by 10% due to a lower external acceleration, $P'_{h\ \max}$ decreases to 7.3 µW for a voltage $U_{C_{\text{tran max}}} = 54$ V, which is much less critical than in the previous case (Fig. 8).

4 Validation trough behavior modeling of the global system

This electromechanical system has been simulated using a mixed VHDL-AMS/ELDO model similar to the one we

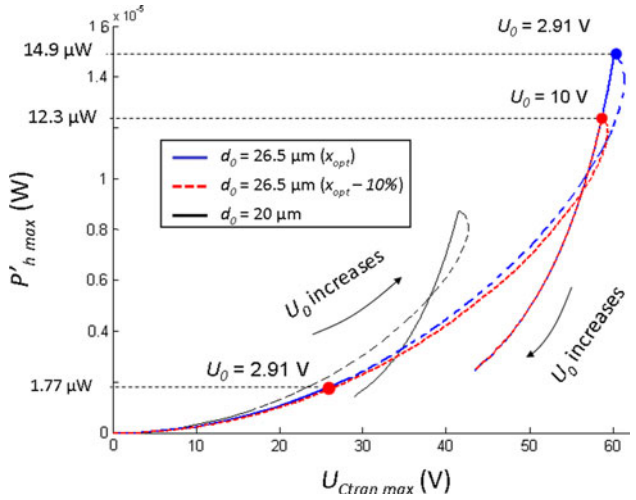

Fig. 7 Evolution of $P'_{h\_\max}$ as a function of $U'_{\text{Ctran}\_\max}$ for an optimized design with a maximal external acceleration and with an acceleration inducing 10% loss of the mobile electrode's displacement

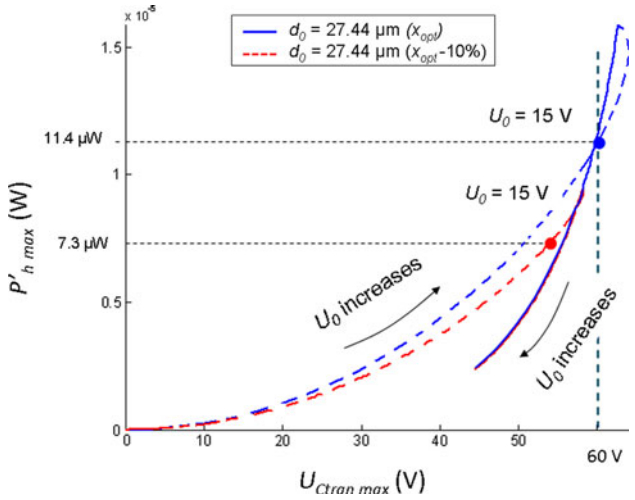

Fig. 8 Evolution of $P'_{h\_\max}$ as a function of $U_{C_{\text{tran max}}}$ for a design optimized with $C_{\max}/C_{\min} = 4$, with a maximal external acceleration and with an acceleration inducing 10% loss of the mobile electrode's displacement

developed in Galayko et al. [3]. To validate the optimization related with the power conversion, the transducer's model has been integrated in an electrical model of the simplified conditioning circuit presented in Fig. 9. The conditioning circuit contains a voltage source generating a DC U_0 voltage and a load allowing to quickly discharge the transducer. Two switches that commutate the transducer's electrodes between the source and the resistance are driven by a control block described in VHDL-AMS. This block achieves a transducer capacitance measurement, and generates short pulses on the switches SW1 and SW2 when the capacitance is maximal and minimal, respectively. Knowing the values of the maximal and minimal transducer's capacitance and the corresponding pre-charge voltage, the energy converted by cycle is calculated from (Eq. 2).

Figure 10 presents the simulated curves highlighting behavior of the optimized transducer for a $C_{\max}/C_{\min}$ ratio of 4. The graph shows the displacement x of the mobile electrode when it is submitted to an external sinusoidal acceleration a_{ext} at the device mechanical resonance. The graph shows also the variations of C_{tran}, $U_{C_{\text{tran max}}}$ and the energy E harvested by the transducer per capacitance variation cycle. On the energy plot, only the curve's envelop is meaningful; it represents the energy harvested after each conversion cycle.

We observe a shift of the median position x_{med} which is due to the shift of the resonance frequency of the resonator when high electrostatic coupling with the spring-mass system occurs [10]. As expected, $U_{C_{\text{tran max}}}$ and the harvested energy increase with the external acceleration. However, the amplitude of the mobile mass vibration first increases then, for higher values of a_{ext} starts to decrease. This is related to the nonlinearity of the electrostatic transducer and in the change of the transducer's impedance when the external acceleration changes. Although this phenomenon was not explicitly taken into account in our analysis, it

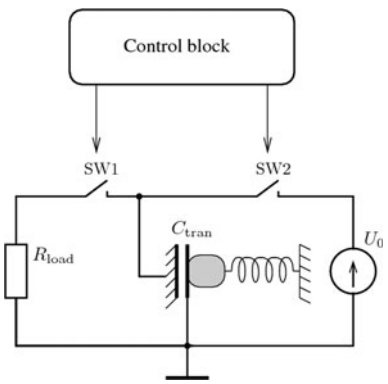

Fig. 9 Simplified conditioning circuit used for validation of the analysis

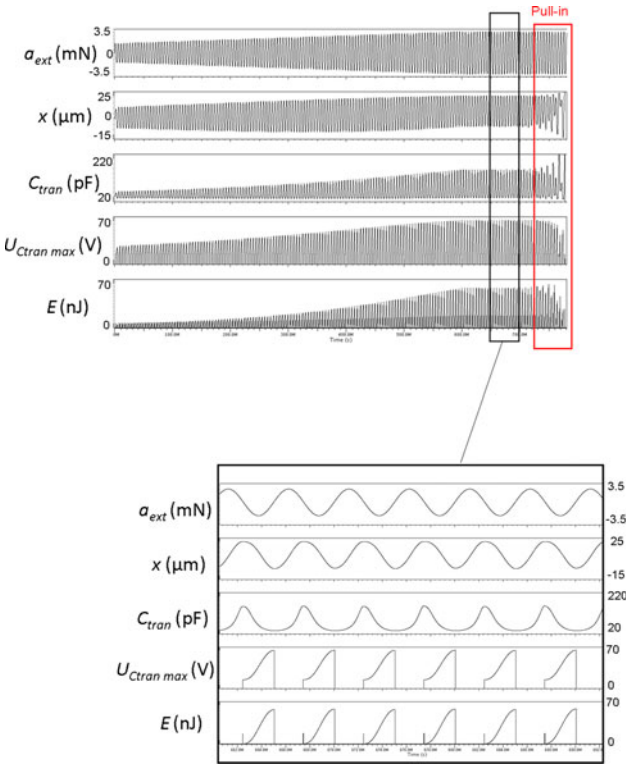

Fig. 10 VHDL-AMS modelling of the optimized OPGC device with a $C_{\max}/C_{\min}$ ratio of four and pre-charged with $U_0 = 15$ V

doesn't come to contradiction with it. It can be seen that for any value of a_{ext}, the mobile mass vibration amplitude and average position are related to the observed $x_{\max}$ in accordance with (Eq. 9) and (Eq. 10). The model used for the transducer is not provided with stoppers, so the pull-in occurs at the end of the simulation. An irregular (non-sinusoidal) motion of the resonator for a_{ext} amplitudes close to the pull-in value can also be observed. This is related with the increased non-linearity of the system in this zone, which unvalidates the model of zero and first harmonic used in this analysis.

When a_{ext} is large enough to allow a maximal displacement of the electrode, $U_{C_{\text{var max}}}$ is saturating at $\sim$60 V. The harvested energy is about 57 nJ so the maximal harvested power is 57 nJ $\times$ 200 Hz $=$ 11.4 µW as predicted in our calculations. If the electrode's displacement is reduced by 10%, the new maximal harvested power is about 7.66 µW. This result matches our calculations with precision below 5%.

5 Conclusion

Vibration Energy harvesting capabilities for an electrostatic transducer having an OPGC architecture have been

presented. We investigated the working principle at constant charge of a VEH pre-charged with a voltage U_0 and submitted to external vibrations. The originality of this work consists in taking into account both electrical and mechanical aspects for the design optimisation, while a constraint on the maximal voltage allowed across the transducer is taken into account in order to preserve the integrity of the conditioning circuit. We detailed how to design the VEH in order to harvest the maximum power when the vibration's characteristics are known.

The proposed mathematical model of the VEH based on accounting only zero and first harmonic is very efficient. It was validated by modeling for the vibration amplitude ranges at which the behaviour of the VEH is regular (periodic and sinusoidal), and it allows to identify the limit of the regular and stable behaviour of the harvester.

This study highlight a fundamental limitation of the VEH with OPGC transducer: with reasonable dimensions required by applications like WSN, smart dust, etc., and MEMS fabrication. The converted power is about 10–20 μW, at frequency 200 Hz. For a given resonator, the main limiting factor is related with the electrostatic unstability (pull-in phenomenon). By varying the stiffness of the spring, or even by getting the spring non-linear, these figures can be increased.

Our results have been validated with a behavioral VHDL-AMS modeling of the OPGC transducer implemented in a simplified conditioning.

Acknowledgments This work has been done in the framework of the project SESAM (Smart Multi-Source Energy Scavenger for Autonomous Microsystems) funded by the French National Research Agency (ANR) through the contract ANR-08-SEGI-019.

References

1. Basset, P., Galayko, D., Mahmood Paracha, A., Marty, F., Dudka, A., & Bourouina, T. (2009). A batch-fabricated and electret-free silicon electrostatic vibration energy harvester. *Journal of Micromechanics and Microengineering, 19*, 115025.
2. Dudka, A., Galayko, D., & Basset, P. (2009). Smart adaptive power management in electrostatic harvesters of vibration energy. In *Proceeding of the 9th international workshop on Micro and nanotechnology for Power generation and energy conversion applications (PowerMEMS'09)*. Washington, USA.
3. Galayko, D., Pizarro, R., Basset, P., Mahmood Paracha, A., & Amendola, G. (2007). AMS modeling of controlled switch for design optimization of capacitive vibration energy harvester. In Proceedings of IEEE international workshop on Behavioral modeling and simulation conference (BMAS'07) (pp. 115–120). San José, USA.
4. Galayko, D., & Basset, P. (2008). Mechanical/electrical power-aware impedance matching for design of capacitive vibration energy harvesters. In *Proceeding of the 8th international workshop on Micro and nanotechnology for power generation and energy conversion applications (PowerMEMS'08).* Sendai, Japan.
5. Galayko, D., & Basset, P. (2010). A general analytical tool for the design of Vibration Energy Harvesters (VEH) based on the mechanical impedance concept—Application to electrostatic transducers. Accepted in TCAS.
6. Meninger, S., Mur-Miranda, J. O., Amirtharajah, R., Chadakasan, A. P., & Lang, J. H. (2001). Vibration-to-electric energy conversion. *IEEE Transactions on Very Large Scale Integration (VLSI) Systems, 9*(1), 64–76.
7. Mitchelson, P. D., Green, T. C., Yeatman, E. M., & Holmes, A. S. (2004). Architectures for vibration-driven micropower generators. *IEEE Journal of Microelectromechancial Systems, 13*(3), 429–440.
8. Nathanson, H. C., Nevel, W. E., Wickstrom, R. A., & Davis, J. R. (1967). The resonant gate transistor. *IEEE Transactions on Electron Devices, ED-14*, 117–133.
9. Roundy, S., Wright, P. K., & Pister, K. S. J. (2002). Micro-electrostatic vibration-to-electricity converters. In *Proceedings of ASME international mechanical engineering congress & exposition (IMECE'02)* (pp. 1–10). Orleans, Louisiana.
10. Yao, J. J., & MacDonald, N. C. (1995). A micromachined, single-crystal silicon, tunable resonator. *Journal of Micromechanics and Microengineering, 5*, 257.

Raphaël Guillemet was graduated in 2006 from the Université Paris-XI (Orsay, France), in the field of applied physics and electronics. He worked 3 years as a research engineer in the research unit CNRS-THALES of Université Paris-Sud. He is currently doing a PhD on silicon-based electrostatic Vibration Energy Harvester at Université Paris-Est/ESIEE Paris.

Philippe Basset has been graduated in electronic from ISEN (Lille, France) and achieved a PhD in electrical engineering from the University of Lille at the Institute of Microelectronics and Nanotechnologies (IEMN, Lille, France) in 2003. After 1 year in Gary Feder's group at Carnegie Mellon University (Pittsburgh, USA) as a post-doc, since 2005 Dr Basset is an associate professor at Université Paris-Est/ESIEE Paris. His research interests deal with energy harvesting from vibrations, temperature gradients and electromagnetic radiations using silicon-based devices.

Dimitri Galayko has been graduated from Odessa State Polytechnic University (Ukraine) in 1998, he received his master degree from Institute of Applied Sciences of Lyon (INSA-LYON, France) in 1999. He made his PhD thesis in Institute of Microelectronics and Nanotechnologies (IEMN, Lille, France) and received the PhD degree from the University Lille-I in 2002. The topic of his PhD dissertation was the design of microelectromechanical silicon filters and resonators for radiocommunications. Since 2005 he is associate professor in University Paris-VI (Pierre et Marie Curie) in the LIP6 laboratory. His research interests include design of integrated analog and mixed circuit and design of integrated interfaces with sensors.

Tarik Bourouina (A'00–M'02-SM'05) received the Diplôme d'Etudes Supérieures (B.S. degree) in physics from the University Houari Boumedienne in Algiers, Algeria, in 1987, the Diplôme d'Etudes Approfondies (M.S. degree) in electronics from the University of Paris-Sud, Orsay, France, in 1988, the Doctorate (Ph.D. degree) in electrical engineering, from the University of Paris XII, Creteil, France, in 1991 and the Habilitation à Diriger les Recherches, from the University of Paris-Sud, Orsay, France, in 2000. From 1991 to 1995, he was a lecturer in the ESIEE Engineering School in Noisy-Le-Grand. In 1995, he joined the University of Paris-Sud, as an Associate Professor in the Institut d'Electronique Fondamentale (IEF), a joint laboratory with CNRS. From 1998 to 2001, he was at The University of Tokyo, as a visiting scientist in the framework of LIMMS. Dr. Bourouina is currently Professor at Université Paris-Est/ESIEE Paris. His current research interests include optical MEMS, microactuators and nanostructures.